Chapter

Refractive Index in Ionic Liquids: Beyond the D Line

Yago Arosa, Carlos Damián Rodríguez-Fernández, Elena López Lago and Raúl De la Fuente

Abstract

In the last decade, the intrinsic tunability of ionic liquids has attracted interest well beyond the disciplines that inaugurated the research on these materials at the beginning of the 1990s. One of these emerging fields is photonics, where the possibility of designing materials with task-specific optical responses is promising for a large number of potential applications. Among the optical properties of ionic liquids, refractive index has been the subject of a thorough investigation because of its relevance in the performance of most optical devices. In this chapter, we address the recent experimental and computational advances on the characterization of the refractive index of ionic liquids and the relations of this magnitude with their structure. Furthermore, we provide an important review of works introducing ionic liquids as essential optical materials in diverse applications.

Keywords: ionic liquids, photonics, optical properties, refractive index, chromatic dispersion, electronic polarizability

1. Introduction

It is well known that ionic liquids (ILs) are very stable ionic materials with a large intrinsic tunability. From the very beginning of the research on ILs, their suitability to be used as designer solvents (or smart materials) was recognized, i.e., the possibility of synthetizing ILs with tailored physicochemical properties to fulfill task-specific requirements. The idea of easily obtaining solvents with specific responses made ILs the subject of an early intensive research in fields as diverse as electrochemistry, catalysis or separation science. Indeed, over the last few years, the tunability inherent to ILs has attracted further attention in new fields, such as photonics.

Designing stable (and non-evaporating liquids) with tailored optical responses is promising for different photonic applications. Among the wide variety of existing optical properties, refractive index is the most fundamental magnitude in any material. In short, it governs the phase velocity of light in a medium and, together with its dispersion; it determines the possible applications of such a material as an optical element. The pioneering measurements of refractive index in ILs were performed as a part of their necessary physicochemical characterization. However, since the possibility of effectively tuning the refractive index in ILs was recognized,

the number of works dealing with this magnitude from an optical perspective has been continuously growing.

In this chapter, the recent research on the refractive index of ILs is reviewed, including the most outstanding experimental and computational milestones in the field. In addition, the basic tools for tuning the refractive index are summarized and some examples of practical implementation of ILs in optical devices are addressed. The short-names used for the ILs mentioned in the text can be consulted in the "Abbreviations" section at the end of this chapter.

2. Experimental determination of the refractive index

2.1 Single-wavelength measurements

A large part of the refractive index measurements in ILs are performed at a single wavelength, the sodium D-line, λ_D = 589.6 nm, as a part of the routinary characterization of the physicochemical properties of new ion combinations or functionalized species. Starting with the pioneering studies by Bonhôte et al. and Huddleston et al. [1, 2], numerous articles were published dealing with the characterization of this magnitude and its dependence on temperature (typically between 293 and 333 K). A representative summary of the research up to 2014 can be found in Ref. [3]. The published data clearly demonstrates the ability to tune the refractive index as a function of the selected counterions, by mixing ILs or dissolving them in other miscible liquids. ILs with refractive indices between 1.60 and 2.08 RIU, comparable to those of optical glasses, were already synthesized in that moment. However, many of them were not transparent in the visible range, which limited their application in imaging or guiding systems.

A few years later, Kayama and co-workers [4] synthesized colorless and transparent ILs with refractive indices greater than 1.60 RIU by combining $[BzC_1im]^+$, $[P_{ppp6}]^+$, and $[C_4C_1imI_2]^+$ cations with $[Sac]^-$, $[Bz\text{-}I\text{-}SO_3]^-$, $[Br]^-$, and $[N(CN)_2]^-$ anions. The strategy followed for the design of these high index compounds was based on the combination of ions with high molar refractions. In this case, they chose to use cations with aromatic structures and to incorporate iodine in the anions.

Other researchers explored the effect on the refractive index of previously unexplored functional groups inserted into the cation. For example, relatively high refractive indices were obtained by Gonfa et al. in 2015 [5] on the next ILs based on the thiocyanate anion combined with: $[C_4C_1im]^+$, $[C_2CNC_4im]^+$, $[C_2CNAim]^+$, $[C_2CNBzim]^+$, and $[C_2CNHeim]^+$. The refractive indices of this set of ILs decreases according to the series: $[C_2CNHeim][SCN] > [C_2CNBzim][SCN] > [C_2CNAim][SCN] > [C_2CNC_4im][SCN] > [C_4C_1im][SCN]$, being their respective values 1.5682, 1.5666, 1.5663, 1.5483, and 1.5391 RIU at 298 K. In this regard, Ullah et al. [6] characterized the IL $[C_2CNC_4im][N(CN)_2]$, which is composed by one of the previous cations paired with a different anion (dicyanamide), in the 293–353 K temperature range. The refractive index values at those temperatures varied from 1.5195 to 1.5061 RIU, being significantly lower than those obtained by replacing the anion by $[SCN]^-$.

Bhattacharjee et al. [7] performed a study in a set of ILs based on the n-alkylphosphonium cations: $[P_{i(444)1}][Tos]$, $[P_{4441}][C_1SO_4]$, $[P_{4442}][(C_2H_5O)_2PO_2]$, and $[P_{8888}][Br]$. The trend observed in the refractive indices is as follows: $[P_{i(444)1}][Tos] > [P_{8888}][Br] > [P_{4441}][C_1SO_4] > [P_{4442}]\ [(C_2H_5O)_2PO_2]$, being their values 1.51233, 1.46912, 1.45983, and 1.48262 RIU at 318 K. Rodil et al. [8] characterized the

refractive index of other phosphonium-based ILs in the temperature range from 283 to 343 K, namely $[P_{4441}][Cl]$, $[P_{4441}][NTf_2]$, $[P_{4441}][C_1SO_4]$, but also $[C_1py][C_1SO_4]$, and $[C_4C_1im][C_1SO_4]$. They observed that the refractive index increased according to the following sequence: $[P_{4441}][NTf_2] < [P_{4441}][C_1SO_4] < [C_4C_1im][C_1SO_4] < [P_{4441}][Cl] < [C_1py][C_1SO_4]$. The values obtained at 293 K are, respectively: 1.4374, 1.4755, 1.4804, 1.5037, and 1.5139 RIU. Hence, cations based on imidazolium or pyridinium species tend to produce ILs with higher refractive index than their phosphonium-based equivalents. On the other hand, Othman et al. [9] focused on ILs based on ammonium cations instead of phosphonium ones. Particularly, they combined diethylammonium and dibutylammonium with alkanoate anions of variable length, $[N_{22}][C_5CO_2]$, $[N_{22}][C_6CO_2]$, $[N_{22}][C_7CO_2]$, $[N_{44}][C_5CO_2]$, $[N_{44}][C_6CO_2]$, and $[N_{44}][C_7CO_2]$. The refractive indices were measured at temperatures ranging from 293 to 333 K. The importance of these liquids lies in their promising ability to absorb CO_2 under typical laboratory conditions. They observed that at 298 K the refractive index varied between 1.43069 and 1.44354 RIU, increasing with the alkyl chain length of the cation and anion.

Lee et al. [10] focused on the so-called Good's buffer ILs (GB-ILs), of potential use in biotechnology thanks to their self-buffering capacity and biocompatibility. Specifically, they studied all the combinations between $[N_{4444}]^+$, $[P_{4444}]^+$, and $[Ch]^+$ with $[MOPSO]^-$, $[BES]^-$, $[TAPSO]^-$, and $[CAPSO]^-$. The obtained refractive indices grow according to the following cationic order: $[N_{4444}]^+ < [P_{4444}]^+ < [Ch]^+$, and the following anionic order: $[MOPSO]^- < [CAPSO]^- < [BES]^- < [TAPSO]^-$. The measured values for the refractive index of these GB-ILs lie in a narrow window (1.47–1.52 RIU) over the entire temperature range employed (288–353 K). On the other hand, Marcinkowski et al. [11] reported refractive index values for ILs based on amino acids, namely they focused in the N-acetyl-L-amino acid ions $[Ala]^-$, $[Val]^-$, $[Leu]^-$, and $[Ile]^-$ combined with the morpholinium-based cations $[Mor_{1,k}]^+$ of variable alkyl chain (k = 2, 3, 4, 6, 8, where k is the number of carbons in the chain). These ILs show low refractive indices, between 1.481 and 1.488 RIU at 318 K.

Khan et al. [12] studied the refractive index of dicationic ILs (DILs) as a further tuning variable. They focused on four ILs based on the $[C_4(C_1im)_2]^{2+}$ cation combined with the anions $[HSO_4]^-$, $[C_1SO_3]^-$, $[OTf]^-$, and $[\rho\text{-}TSA]^-$. Refractive index values were measured in the temperature range from 293 to 323 K. The decreasing order of refractive indices of these DILs is: $[C_4(C_1im)_2][OTf]_2 > [C_4(C_1im)_2][HSO_4]_2 > [C_4(C_1im)_2][C_1SO_4]_2 > [C_4(C_1im)_2][\rho\text{-}TSA]_2$. The lowest value is shown by $[C_4(C_1im)_2][OTf]_2$ while the highest value is that of $[C_4(C_1im)_2][\rho\text{-}TSA]_2$, whose anion exhibits larger aromaticity and bulkier structure than the rest. In addition, and according to literature, the values of the refractive indices for these DILs are higher than their monocationic equivalents. For instance, the values of the refractive indices of $[C_4C_1im][C_1SO_3]$ and $[C_4C_1im][OTf]$ are, respectively, 1.4792 and 1.4368 RIU, which are lower than those of $[C_4(C_1im)_2][C1SO_3]_2$ and $[C_4(C_1im)_2][OTf]_2$.

As depicted by the previous works, a large part of the research on refractive index has been done in neat ILs. However, some authors focused on mixtures of ILs with other solvents. A relevant contribution is that of Branco et al. [13], who determined the refractive index of index of four ILs: $[C_6C_1im][NTf_2]$, $[C_{10}C_1im][NTf_2]$, $[C_4C_1im][N(CN)_2]$, and $[P_{666,14}][N(CN_2)]$: mixed with Poly(ethylene glycol) 200 (PEG 200) at 298 K. They obtained refractive index values between 1.5096 and 1.4311 RIU. These measurements were combined with existing volumetric data to obtain molar refraction at different mole fractions. They showed that the molar refraction is highly

dependent on molar volume although it follows a linear trend upon mixing. Oppositely, they also show that the refractive index follows a nonlinear trend with the molar composition of the mixture. Other important work is that of Wang et al. [14], who studied the refractive index of an asymmetrical DIL, $[piC_5py][NTf_2]_2$, and its binary mixtures with acetonitrile at temperatures from 293 to 323 K. In this case, the achieved refractive index range goes from 1.3297 to 1.4514 RIU.

2.2 Wavelength-dependent measurements

Although most refractive index measurements in ILs concern λ_D, it is increasingly common to find articles aimed to determine this magnitude over broader bands in the visible range and adjacent spectral regions. These wavelength-dependent measurements are spurred by the emergence of different optical applications (see Section 4), in which material chromatic dispersion, the derivative of the refractive index with respect to wavelength, is of crucial importance. Since ILs usually present high absorption below 300 nm, these measurements often concern longer wavelengths in the UV, the whole visible region and the NIR up to about 2 microns.

To our knowledge, the first refractive index measurements of ILs at different wavelengths were performed in 2011 by Calixto and co-workers [15]: they studied six ILs, mainly from the imidazolium family, at six wavelengths in the range of 400–650 nm. The authors indicate that they used a spectroscope to carry out the measurements, but do not give further details about the apparatus. In 2014, Novoa et al. [16] used a multi-wavelength Abbe refractometer (Atago DR-2) to measure the refractive index of a set of five ammonium-based and five 1-butyl-3-methylimidazolium-based ILs at six wavelengths in the 475–680 nm range. Interpolation of these data using a Cauchy dispersion formula allowed them to determine the refractive index at other wavelengths in that range.

In 2017, Chiappe et al. [17] performed systematic studies of wavelength-dependent refractive index in 1-alkyl-3-methylimidazolium-based ILs, with alkyl chains of length k = 1, 4 and 6, combined with three phosphorus-containing anions, $[(C_1)_2PO_2]^-$, $[C_1C_1OPO_2]^-$, and $[C_1OHPO_2]^-$. Measurements were performed at five wavelengths (450, 532, 632.8, 964, and 1551 nm) in the temperature range from 353 to 443 K using prism coupling as the method for the refractive index determination. A linear decrease of refractive index with temperature was observed, meaning that the thermo-optic coefficient, which is the variation of refractive index with temperature, dn/dT, is constant in the measuring range. Regarding dispersion, typical curves of decreasing refractive index with increasing wavelength were obtained (normal dispersion) and the refractive index values within the spectral region of interest were interpolated at T = 393 K using a five-term Cauchy equation:

$$n^2(\lambda, 393\,K) = A_0 + A_1\lambda^2 + \frac{A_2}{\lambda^2} + \frac{A_3}{\lambda^4} + \frac{A_4}{\lambda^6}, \tag{1}$$

while, for temperature, they considered the following dependence:

$$n(\lambda, T) = n(\lambda, 393\,K) + (T - 393\,K)\frac{dn}{dT}. \tag{2}$$

Regarding the structure of the ILs, the authors observed that, for these particular ILs, refractive index decreases with the length of the alkyl chain of the imidazolium

cation. Furthermore, they investigated the effect of each anion on refractive index by means of *ab-initio* calculations.

The same group and using the same method [18] measured the dispersion of seven ILs of the levulinate family, also at the same wavelengths and at a similar temperature range. In this case, the interpolation of the dispersion curves was done using the Sellmeier relation:

$$n^2(\lambda, T) = 1 + \frac{S(T)\lambda^2}{\lambda^2 - \lambda_{uv}^2} + d \cdot \lambda^2, \tag{3}$$

with a linear relationship of S on T. They also determined the group index, which is defined as $n_g(\lambda) = n - \lambda \frac{dn}{d\lambda}$. At the microscopic level, the dependence of the electronic polarizability on λ and T was analyzed.

Wu et al. [19] applied ellipsometry to measure the refractive index of six commercial ILs with values around 1.40 RIU ([C_4C_1im][PF_6], [C_4C_1im][BF_4], [C_4C_1im][NTf_2], [C_4C_1im][OTf], [$P_{666,14}$][NTf_2], and [$P_{666,14}$][Cl]) in addition to two high refractive index ILs (n > 1.70 RIU): [C_2C_1im][BrI_2] and [C_2C_1im][I_5]. Employing this technique allowed them to measure the extinction rate associated to absorption. For the low refractive index ILs, they used a two-term Sellmeier relation to describe their material dispersion. They did not use any relationship for the high refractive index ILs, as the dispersion curve was more complex as a consequence of the higher value of the extinction coefficient. Furthermore, these authors demonstrated that the evaluated ILs can be used as immersion liquids in photonic crystals. Also using ellipsometry, Rola et al. [20] measured the refractive index of solid layers of three polymerized ILs, [$AllC_1$im][Cl], [$AllC_1$im][NTf_2], and [$AllC_1C_1$im][NTf_2]. These layers were fabricated by electron beam patterning to be used as planar photonic microcomponents. The refractive indices of the neat ILs were also measured, but, in this case, using a spectroscopy-based method. Indeed, what they did was to study the interference patterns produced by the liquids when introduced within a commercial micrometer-thick cuvette. The refractive index curves of both neat and polymerized ILs were fitted using a three-term Cauchy relation in the spectral range from 300 to 1100 nm. The authors observed that polymerization increases the refractive index from values lower than 1.6 RIU to higher values (increments in the range 0.1 to 0.4 RIU).

Spectroscopic techniques were also used by Elmahdy [21] to measure the refractive index of two ILs, [C_4C_1im][BF_4] and [C_4C_1im][OTf]. Transmittance (T) and absorbance (A) measurements in the spectral range from 200 to 1100 nm allowed the determination of the refractive index as follows:

$$n = \frac{1+R}{1-R} + \sqrt{\frac{4R}{(1-R)^2} - \kappa^2}, \tag{4}$$

with κ being the extinction coefficient and $R = 1 - \sqrt{Te^A}$. For both ILs, they observed a refractive index maximum caused by an absorption peak located around 300 nm. In order to reproduce the curve, they made different fits for wavelengths below and above this absorption maximum.

De la Fuente group made extensive use of a technique called Refractive Index Spectroscopy by Broadband Interferometry (RISBI), in which the spectral interference between a beam passing through a cell with the sample and a reference beam is

resolved. In 2017, they measured the refractive index of 14 ILs belonging to the imidazolium family [22]. The spectral range of measurement was between 400 and 1000 nm and the temperature was kept constant at 300 K. A five-term Cauchy relation, similar to that of Eq. (1), was used to describe the refractive index curves. The absorption of water by the samples was taken into account, considering the solution as an ideal binary mixture in which the refractive index is given by Newton's equation.

In 2018 the studies continued [23], this time considering a temperature range from 298 to 323 K. In this case, the ILs were divided into four different groups according to their common cations or anions. This arrangement allowed them to analyze the dependence of the refractive index on the length of the alkyl chain of the cation. On the other hand, they employed a single-term Sellmeier formula, similar to that of Eq. (3), to fit the refractive index curves. Using this expression, the authors were able to recognize that the variations of the squared refractive index with temperature and wavelength are independent. In addition, the resonance wavelength of the model turned out to be independent of both alkyl chain length and temperature.

Their work continued in 2020, material dispersion was considered for 20 different ILs and the characterization was extended by incorporating the analysis of higher order dispersion and the thermo-optic coefficient dependence on wavelength [24]. Furthermore, in other work [25], the spectral range of measurement was further increased to include the region from 300 to 1500 nm, as shown in **Figure 1**, while still considering different temperatures within the interval of 293–313 K. In order to fit the refractive index curves in such a broad spectral range, it was necessary to use a Sellmeier dispersion relation with three terms. Again, the authors observed that the wavelengths of resonance were independent of temperature and alkyl chain length:

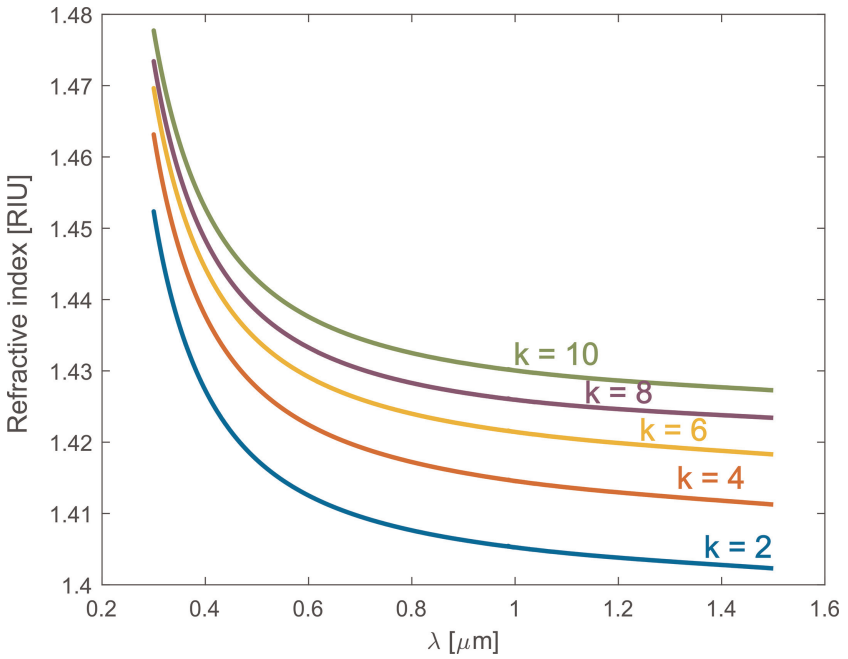

Figure 1.
Refractive index of the $[C_kC_1im][BF_4]$ family of ILs for alkyl lengths of k = 2, 4, 6, 8, and 10 in the spectral range of 300–1500 nm at 298 K. Data extracted from Ref. [25].

$$n^2(\lambda, T) = 1 + \left(c_1' + c_1''\Delta T\right)\frac{\lambda^2}{\lambda^2 - \lambda_1^2} + \frac{c_2\lambda^2}{\lambda^2 - \lambda_1^2} + c_3\lambda^2. \quad (5)$$

To analyze the dependence of the refractive index on the alkyl chain length (k), the Lorentz-Lorenz equation was considered:

$$R(\lambda, k) = V(T, k) \cdot \frac{n^2(\lambda, T, k) - 1}{n^2(\lambda, T, k) + 2}, \quad (6)$$

where R is the molar refraction of the IL and V its molar volume. With this expression, the temperature dependence of refractive index was separated from the spectral dependence. This was possible because the thermal contributions arise from the changes of molar volume with temperature (thermal expansion coefficient) while the spectral ones arise from the dependence of electronic polarizability on wavelength. Furthermore, the authors determined that both parameters vary linearly with k.

3. Predictive models

3.1 Prediction based on empirical models

Empirical models are intensively used in the field of ILs to complete the gaps within the available experimental data and to compare disparate compounds. These models, which at times bereft of a theoretical underpinning, venture into the realm of fitting to faithfully represent values through the utilization of elementary equations, such as linear fits or low-order polynomials.

Works dealing with empirical prediction of wavelength-dependent refractive index are limited to Sellmeier formulas and Cauchy relations within the spectral range of measurement. In contrast, the temperature-induced variation of the refractive index finds more extensive documentation within the extant literature. Multiple researchers not only articulate refractive index values along the λ_D at sundry temperatures but also engage in the calculation of the thermo-optic coefficient. This coefficient, generally dependent on temperature for a given material, lends itself to approximation within a confined dynamic range through linear regression, notably applicable to a large number of ILs.

Concurrently, important efforts are done to investigate the correlation between these adjustments and the chemical architecture of ILs. The work by Gardas et al. [26] serves as a compendium, presenting diverse thermo-physical properties modeled through semi-empirical fits, among them, the variation of refractive index with temperature. This group proffers a model to predict the refractive index of ILs which is encapsulated by:

$$n_D = A_{nD} - B_{n_D}T, \quad (7)$$

where the coefficients A_{n_D} and B_{n_D} aggregate the contributions of molecular blocks defined by the authors (cations, anions and carbons in alkyl chains). This analytical pursuit, echoed in other works such as those of Sattari et al. [27] and Ullah et al. [6], exemplifies a kind of strategy based on building the refractive index (and other physicochemical properties) from the contribution of molecular fragments.

Notably, Gardas et al. refrain themselves from an explicit development to discern the impact of each type of fragment in the thermo-optic coefficient. This subsequent elaboration, possibly arising from the theoretical derivation (as alluded to in the text), illuminates the limited influence of polarizability on the thermo-optic coefficient, with the latter predominantly governed by the coefficient of thermal expansion [25]. Despite the foregoing, Gardas' investigation exhibits the occasional sufficiency of an empirical model. Deviations ascertained for a cohort of 24 imidazolium-based ILs reveal relative deviations in refractive index below 0.5% for the 93% of the values.

3.2 Prediction based on electronic polarizability and the Lorenz-Lorenz equation

Semiempirical models are useful ways to rationalize the measurements of refractive index in ILs. However, while the resources to conduct experimental research are limited, the number of possible ion combinations is virtually infinite. For this reason, simulations are especially powerful tools to study the refractive index in these materials. The strategies for computing the refractive index of ILs are diverse, however, they are always based on one of these two approaches: (i) finding the electronic polarizability and using the Lorentz-Lorenz equation to obtain the refractive index or (ii) training an algorithm with experimental refractive indices to predict the refractive index of new species. All the strategies based on electronic polarizability have in common that they exploit the additivity of this magnitude in terms of atoms, molecular groups or ions. However, electronic polarizability can be obtained following very different paths. A large number of works obtain it from *ab initio* calculations based on Density Functional Theory (DFT) or Møller-Plesset Perturbation theory (MP), while others rely on obtaining it from the statistical analysis of experimental data.

Possibly, the work of 2009 of Izgorodina et al. [28] is the first one comparing experimental refractive indices with *ab initio* predictions derived from static electronic polarizabilities (wavelength independent) and molecular volumes. The work itself is not devoted to refractive index but to explore the possible existence of an ionic polarization component in the dielectric constant of ILs. Despite it, they showed that the experimental refractive index at λ_D can be approximately estimated by using the Lorentz-Lorenz equation, Eq. (6), and assuming that the electronic polarizability of the IL is approximately that of the composing ions.

Some years afterwards, in 2013, Bica et al. [29] published the first work completely focused on the estimation of the refractive index by means of computational methods. In this case, the electronic polarizability data was obtained from statistical analysis using the Lorentz-Lorenz equation and experimental refractive indices (at λ_D) and densities. The authors assumed atomic additivity in both electronic polarizability and molar volume, and performed a designed regression analysis to obtain the contributions of individual atoms to these magnitudes. From them, they estimated the electronic polarizability, molar volume and refractive index of a huge number of imidazolium-based ILs. While this model is restricted to ILs containing the imidazolium cation, it is able to provide refractive index with a mean absolute deviation of 0.0035 RIU. Indeed, deviation is lower for most of the ionic combinations, but the overall performance of the model is hindered by its limited ability to reproduce the refractive index of ILs containing the dicyanamide anion.

Another important result of the same work of Bica et al. is that it explains why in some ILs the refractive index rises with the length of alkyl chains while, in others, the trend is the opposite. According to the authors, the key parameter to explain these different behaviors is the Molecular Polarizability Density (MPD) of the -CH_2- unit.

The MPD is nothing more than the ratio between electronic polarizability and volume in a molecular fragment or molecule, $MPD = \alpha_{mol}/V_{mol}$. In accordance with the Lorentz-Lorenz equation, Eq. (6), this ratio is just what determines the value of the refractive index in a liquid. For -CH_2- units, it is 0.0661, in the CGS system (dimensionless) or 7.3546×10^{-12}, C V^{-1} m^{-1} in the SI system. When the MPD of the combination of a cation and an anion is lower than that of the -CH_2- units, increasing the length of an alkyl chain rises the overall MPD of the IL and increases the refractive index. It is the case, for instance, of imidazolium-based cations combined with $[BF_4]^-$, $[PF_6]^-$ or $[NTf_2]^-$ anions. Oppositely, when the combination has higher MPD than that of the -CH_2- units, increasing the alkyl chain length diminishes the refractive index, as it happens in imidazolium-based cations paired with alkyl sulfates or dicyanamide anions.

In 2016, Bernardes et al. [30] published a continuation of the work of Bica addressing its limitations in predicting the refractive index of dicyanamide-based ILs. According to the authors, the worse performance of their model with these anions was because carbon hybridization was not taken into account, cursive, all carbons were assigned with the same electronic polarizability. Hence, in this new work, the authors expanded the set of ILs upon study beyond imidazolium-based combinations, and allowed the designed regression to distinguish between different types of carbon hybridization (sp, sp^2 and sp^3). The result was a model which was able to predict the refractive index at λ_D and the mass densities of ILs more accurately than that of Bica, with good performance on dicyanamide anions and pyridinium cations. It is worth to mention that the authors also checked the effect of considering hybridization in N and S atoms. However, they found no evidence of improvement in the refractive index prediction while the regression analysis became more complex. They also compared the atomic polarizability values derived from this model with those predicted by quantum mechanical calculations at the levels of theory MP2/augcc-pVDZ and CCSD(T)/aug-cc-pVDZ. The results revealed that their designed regression overestimates the polarizability in cations and underestimates it in anions because of the lacking/extra electron in those types of ions. However, since ILs are composed by both anions and cations, these errors counterbalance and the calculation of electronic polarizability in ionic pairs is unaffected.

In 2018, Heid et al. [31] explored the possibility of designing ILs with refractive indices higher than 2.0 RIU by using polyhalide anions. For doing it, the authors performed a new designed regression to include halides in the set of atomic polarizabilities derived by Bernardes et al. In their regression, they employed experimental refractive indices at λ_D of 55 halide-containing ILs while keeping constant the polarizabilities of the atoms already derived by Bernardes. In other words, the only fitting parameters were the polarizabilities of the halide atoms, Cl, Br, and I. The validity of the derived polarizabilities was successfully tested against quantum mechanical calculations at the M06-2X/Sadlej level of theory. The authors concluded that the MPD of iodide anions is the highest one among the considered halides, which means that iodide-based polyhalide anions are the best option to increase the value of refractive index. Indeed, they predicted that the refractive index of ILs based on combinations of common cations such as ammonium or imidazolium with polyiodides can easily go beyond 2.0 RIU.

More recently in 2020, Rodríguez-Fernández et al. [25] employed a semi-empirical approach to predict the refractive index in ILs as a function of both wavelength and temperature. The key idea is exploiting that the thermal and dispersive contributions to refractive index are independent in the Lorentz-Lorenz equation, Eq. (6).

The method requires knowing the experimental density of the IL at the desired temperature (molar volume, thermal dependence) and computing its wavelength-dependent electronic polarizability (dispersion). Specifically, the calculations in this work were done using the Coupled Perturbed Kohn-Sham (CPKS) method at the B3LYP/6-31++G(d,p) level of theory. The performance of this approach was evaluated comparing the predictions of the model with experimental data of 1-alkyl-3-methylimidazolium tetrafluoroborate-based ILs. The simulated refractive indices presented a relative root-mean square deviation of 0.4% in the thermal range from 293 to 313 K and the spectral range from 300 to 1500 nm. Hence, the authors confirmed that predictive models based on splitting the thermal and dispersive contributions to refractive index are able to provide accurate values for this magnitude.

In 2022, Rodríguez-Fernández et al. [32] published a new model for the fast prediction of the refractive index in ILs together with an atlas of the expected values for more than 1000 ion combinations. The method was developed to obtain accurate refractive indices at T = 298 K and λ = 589 nm by means of *ab initio* calculations of electronic polarizability (CPKS method) and molecular volumes on isolated ions. According to the authors, they were able to predict the refractive index of the 75% of the compounds in their test set (71 ILs, including imidazoliums, piperidiniums, pyrrolidiniums, pyridiniums, etc.) with an absolute error below 0.02 RIU. The level of theory employed was the B3LYP/6-31++G(d,p), chosen after testing other possibilities because its good performance/computational cost ratio.

In their model, electronic polarizability was additive in terms of ions, $\alpha_{IL} = \alpha_{anion} + \alpha_{cation}$, but not molecular volume, which requires a more delicate treatment given by: $V_{IL} = f_{scale}(V_{cation} + V_{anion}) + f_{int}(V_{cation} + V_{anion})^2$. In this expression, the f-terms are empirical parameters obtained by comparing experimental molecular volumes and *ab initio* predictions. f_{scale} mimics the effect of temperature and cavity volume in bulk ILs (DFT is performed at 0 K and in gas-phase), and f_{int} represents the packing ability and interactions of the ions. Note that the volume correction can be applied to single ions (a counterion is not required), hence, the MDP expected for isolated ionic species ($MPD = \alpha_{mol}/V_{mol}$) is also affected by this correction.

Using this volume correction, the authors showed that the species presenting charge delocalization tend to have largest MPD values than those which are aliphatic. In order to shed some light on this trend, they performed electronic polarizability calculations on an imidazolium cation with a conjugated chain of variable length. The simulations showed that electronic polarizability grows faster than expected from the linear addition of atomic polarizabilities in the chain, i.e., it becomes nonlinear. This finding is closely related to the effect of carbon hybridization in electronic polarizability shown by Bernardes et al., since sp^2 carbons in ILs often appear as a part of conjugated molecular regions. Last but not least, the authors pointed out that tuning charge delocalization in IL is a powerful tool to obtain liquids with refractive indices beyond 2.0 RIU.

Also in 2022, Koutsoumpos et al. [33] published a work aimed to predict the refractive index (or the mass density) of ILs by combining the electronic polarizability model of Wildman-Crippen and the Lorentz-Lorenz equation. The Wildman-Crippen model [34] was published in 1999 and it is based on assuming that electronic polarizability is an additive magnitude in terms of atomic contributions that are sensitive to aromaticity and chemical environment. Koutsoumpos et al. showed that using the atomic polarizabilities of Wildman-Crippen and combining them with experimental density measurements, the refractive index of ILs can be estimated with absolute errors as low as 0.002 RIU.

3.3 Artificial intelligence applied to refractive index prediction

In the realm of predicting the refractive index and its variations with different magnitudes, a recent and compelling approach involves the use of Artificial Intelligence (AI) learning systems. These methods have garnered significant attention, particularly with the development of specialized accelerators in various fields. The study of ILs is no exception, and, in recent years, there has been a proliferation of articles focused on the application of different AI techniques for analysis. This type of investigation closely aligns with semi-empirical models in terms of addressing the problem by using known magnitudes (such as chemical structure or other thermophysical properties) to predict the refractive index of materials.

In the context of predicting the refractive index of ILs, AI techniques, including machine learning models, have been employed to establish correlations between the molecular structure and optical properties. This involves training models on datasets containing information about the molecular features of various ILs and their corresponding refractive indices. Researchers frequently leverage computational chemistry methods, molecular descriptors, and advanced machine learning algorithms to construct accurate predictive models. These models contribute to a deeper understanding of the structure-property relationships that govern the optical behavior of ILs, thereby facilitating the design of innovative compounds with customized optical characteristics. They can be broadly categorized into two main groups: unsupervised models, which focus on identifying Principal Components (PCs) and reducing dimensionality for predictions, and supervised models, which predict the refractive index based on extensive databases.

While unsupervised learning is less commonly employed in predicting specific properties such as refractive index, it still finds utility in the pre-processing and exploratory phases of analysis, contributing to a comprehensive understanding of ILs. Unsupervised clustering techniques, including k-means clustering, hierarchical clustering, and density-based clustering, can be applied to unveil patterns or groups within the data. In addition, techniques such as Principal Component Analysis (PCA) or t-distributed stochastic neighbor embedding (t-SNE) serve to reduce data dimensionality, enhance visualization, and potentially optimize subsequent modeling efforts.

A notable example of the application of unsupervised models in the analysis of ILs is presented by the work of Venkatraman et al. [35], where researchers explore the main contributors influencing the refractive index using four different optimization routines available in the statistical software R. Tree-based approaches are reported to yield the best results, exhibiting a mean absolute error lower than 0.01 RIU for a set of 14 ILs.

Despite the effective performance of these models, the identification of the main contributions proves to be challenging. Venkatraman et al. addressed this task through PCA. PCs represent linear combinations of initial inputs, emphasizing the variables, such as temperature, with the greatest influence in the variation of the refractive index. The orthogonality of these PCs ensures minimal covariance, thereby reducing dimensionality. In the aforementioned work, the first two PCs accounted for 50% of the refractive index variance, demonstrating a successful reduction in complexity. Notably, these two PCs are predominantly influenced by descriptors related to the anion and cation, encompassing factors such as geometry, energy levels, gauge, and core-core repulsion. This approach demonstrates the capability of unsupervised models to classify ILs without prior knowledge and streamline the system into a more manageable PCs problem.

Beyond classification, the authors analyzed the influential variables on the refractive index using four different supervised routines (PLSR, GBM, Cubist, and RF). Notably, the models with superior system descriptions (Cubist and RF) highlight temperature as a crucial variable affecting refractive index variance. These studies contribute to narrowing the scope of dispersion studies of ILs by benchmarking their chemical and structural properties. However, it is essential to note that the absolute errors observed, even in the best models, are close to 0.01 RIU, suggesting the need for further refinement in predictive modeling.

In contrast to the previously discussed unsupervised models, supervised models predict the refractive index or polarizability of ILs based on molecular structure. These approaches are commonly known as Quantitative Structure-Property Relationship (QSPR) models, where "structure" typically refers to the arrangement of atoms in a molecule, while "property" encompasses specific chemical or physical characteristics, such as boiling point, solubility, toxicity, or refractive index.

Within this category, machine learning algorithms (Random Forests, Decision Trees, SVM, Neural Networks) are widely employed in ILs because of the descriptors used. Supervised methods require a labeled dataset with input features (descriptors) and corresponding target values (refractive indices) for training. However, a significant challenge arises from the unbalanced nature of these datasets, as specific ILs, usually those commercially available, are extensively studied, whereas others are only sporadically addressed. As depicted in **Figure 2** from Esmaeili et al. [36], the experimental data available is largely dominated by three cations (∼80%) and a notable prevalence of the $[NTf_2]^-$ anion (∼28%).

In the context of this approach, recent studies by Esmaeili et al. [36] and Baskin et al. [37] delve deeply into multiple widely used machine learning algorithm models and compare their utility. These studies utilize thousands of data points to develop models and conduct performance tests for various routines. In these cases, the input variables are not PCs calculated from unsupervised algorithms but rely on theoretical

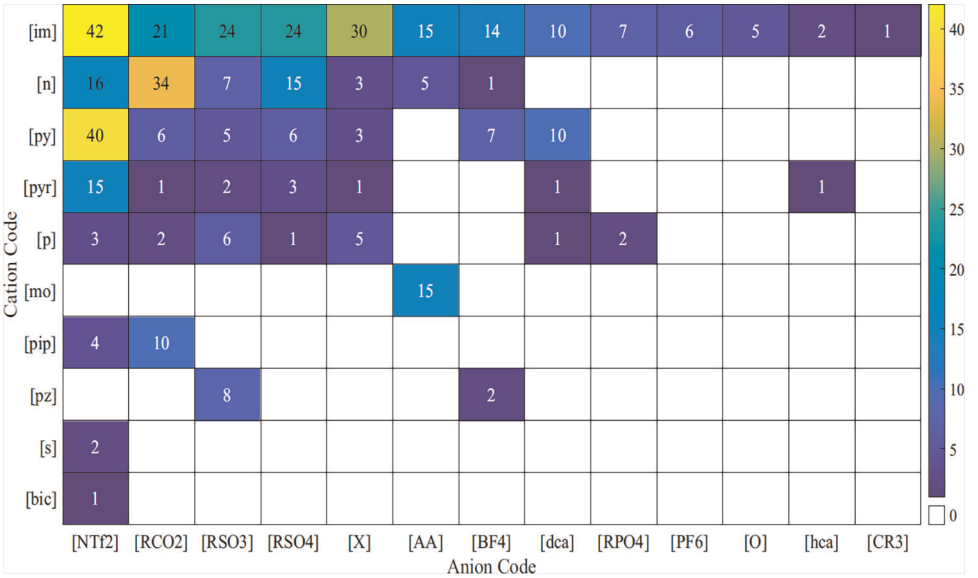

Figure 2.
Number of experimental entries employed by Esmaeili et al. for each type of IL as a function of their composing cations and anions. The figure was extracted from their work [36].

models based on the chemical structure of molecules, similar to those from Ref. [34]. Esmaeili et al. achieved outstanding performance in some routines (R^2 = 0.9973 for CatBoost), even incorporating wavelength-dependent values, although some conclusions remain debatable.

Two key insights emerge from these works that contradict previous studies. First, the influence of temperature and wavelength on the refractive index is downplayed in favor of structural variances, whereas PCA demonstrated a clear dominance of temperature over other chemical variances. The debate on this issue arises because of the wide range of thermo-optic coefficients and chromatic variations observed in ILs (refer to the experimental section). Second, the increase of the alkyl chain in imidazolium-based ILs is considered to always produce a increase in the refractive index. This contradicts findings discussed in studies such as those from Ref. [29], indicating that the refractive index can decrease with increasing alkyl length for a given anion in imidazolium-based liquids.

In a broad perspective, we can optimistically view AI as a powerful tool for refractive index analysis. Its synergy with computational models may highlight specific features crucial for refractive index tunability and enable reasonable prediction of their values. However, there is a long road ahead, with many analyses showing a non-negligible survivorship bias due to the concentration of experimental data on a limited set of liquids. Furthermore, the lack of experimental values for chromatic dispersion poses a challenge to these models, significantly limiting their performance.

4. Applications

Ionic materials, especially liquids are excellent candidates to be part of a new generation of photonic materials [38], with their recognized tunability being highly valued. Although the optical properties of ILs have been studied for the last 20 years, the most important advances at the fundamental and applied level have been made in the last decade, although there is still a long way to go to technologically consolidate them in the field of photonics.

Early published works presented ILs as potentially efficient materials for incorporation into devices operating in extreme climatic conditions. For example, they have been proposed as the basis of liquid mirrors for lunar telescopes [39] due to their low vapor pressure and their ability to remain liquid at temperatures as low as 130 K; or as optical thermometers [40] because they do not evaporate at temperatures reached in extremely hot regions such as some deserts.

Their potential application in optical mineralogy became apparent very early [41] as an alternative to the currently available high-index immersion fluids, which are volatile, toxic, or both. Recently, they also have been proposed as immersion liquids for filling porous materials, such as photonic crystals. In particular, in Ref. [19], ILs with high ($n_D > 1.7$ RIU) and low ($n_D < 1.5$ RIU) refractive indices were employed as immersion liquids to tune the optical properties of photonic crystals or to tune the refractive indices of the materials constituting these photonic crystals. Another remarkable implementation is the one of Guo et al. in Ref. [42]. They introduced an IL in a microstructured optical fiber to perform all-optical control of light transmission. For doing it, they exploited the dependence of the refractive index of the IL on temperature to modify the bandgap of the fiber and to control the attenuation through the system.

Subsequently, taking advantage of the influence of the refractive index on parameters such as group index or group velocity dispersion, Abood et al. [43] designed and

computationally optimized a *Coupled-Slot Slab Photonic Crystal Waveguide*-based device to obtain slow light guided modes by filling parts of the structure with polymerized ILs of different refractive indices (1.3–2.1 RIU). The final device had high group index (low group velocity), a broad bandwidth and a wide spectral range with zero dispersion. The infiltration of the IL in the optimized device (for n = 1.8 RIU) improved its performance by reducing the bit length from 4.6748 to 4.2817 μm, increasing the bandwidth from 102.78 to 126.09 nm, the normalized delay bandwidth product from 0.663 to 0.724, the bit rate from 3.2 to 3.93 Tb/s and the average buffer capacity from 213.912 bits to 233.553 bits. Conversely, the group rate was reduced from 10.3 to 8.9 and delay times from 34.66 to 28.8 ps.

Sensors incorporating ILs in their composition have also been developed in recent years. In Ref. [44], a capacitive-type pressure sensor consisting in a porous polyvinylidene fluoride (PVDF) film sandwiched between two transparent electrodes is proposed. By filling the pores with an IL of the same refractive index as the PVDF, the transmittance of the film increases dramatically from 0% to 94.8% in the visible range. In addition to optical adaptation, the IL also significantly improves signal intensity and sensitivity due to the formation of an electrical double layer at the dielectric-electrode interfaces. Furthermore, it also enhances the hardness and elasticity of the active material due to a plasticizing effect. This sensor exhibits high flexibility, 90.4% transparency, a sensitivity of 1.19 kPa^{-1} and a low detection limit of ≈0.4 Pa, combining well the properties of flexibility, transparency, and detection.

Liquid-core fiber optic sensors filled with $[C_2C_1im][Ac]$ and $[C_4C_1im][Ac]$ have also been implemented to evaluate their suitability for CO_2 detection [45]. The CO_2 absorption in the liquids manifested in a reduction of refractive index (very similar in both ILs) and transmittance (attributed to the existence of scattering generated by the CO_2 bubbles).

Other field where the knowledge of the refractive index dispersion of ILs is essential is optofluidics, since it is required to design achromatic liquid lenses or dispersive prisms. Early research in this field developed variable focal liquid lenses [15, 46–48]. In these works, the focal length of the lens is controlled with pressure, electric field or by changing the filling liquid. Hu et al. used electrowetting to vary the curvature of the meniscus formed at the interface between two immiscible liquids, in this case an IL and dodecane. They tested ILs of the imidazolium family that span a refractive index range between 1.4089 and 1.5329 RIU: $[C_2C_1im][ClO_4]$, $[C_4C_1im][ClO_4]$, $[C_4Py][BF_4]$, $[C_2C_1im][NTf_2]$, $[C_2C_1im][N(CN)_2]$, $[C_4C_1im][OTf]$, $[C_4C_1im][NO_3]$, $[C_2C_1im][BF_4]$, and $[C_4C_1im][PF_6]$. Varying the applied voltage from 0 to 95 V, they obtained different focal distances from −1.5 to +1.5 m using the aforementioned liquids. To achieve significant focal changes, voltages above 60 V had to be applied.

Continuing with the fabrication of lenses, Calixto et al. [46] proposed the use of ILs for producing liquid microlenses in a polymer matrix. They used $[C_2C_1im][BF_4]$, $[C_4C_1im]$ $[BF_4]$, $[C_2C_1im][NTf_2]$, $[C_4C_1im][NTf_2]$, $[C_2C_1im][CF_3COO]$, and $[C_4C_1im][CF_3COO]$ mixed with other solvents to achieve a wide range of refractive index variation and, hence, focal lengths. A few years later, Calixto et al. [15] designed an achromatic varifocal multichamber lens based on the three-chamber design of Reichelet and Zappe. For this purpose, they used ILs with high and low Abbe number. The focal length is modified by varying the amount of liquid/pressure in the chambers. Authors in Ref. [49] proposed a similar structure that also allowed the size of the two chambers to be varied by injecting or withdrawing liquid, simplifying the zoom function and minimizing aberrations.

There are also studies exploring the use of ILs in electro-optical devices by investigating the variation of the refractive index and the appearance of birefringence when an electric field is applied. In Ref. [50], a little more knowledge is advanced by trying to understand the mechanisms that lead to the modification of the refractive index in the transverse direction to the application of the field and, consequently, to the variation of the focal length of a lens formed by the IL $[C_8C_1im][NTf_2]$. The authors related the refractive index gradient to modest changes that occur in the surface charge density, resulting in a free charge density gradient in the liquid. They estimated the thermal effects on the refractive index generated by the Joule effect, whose contribution is much smaller than that of the applied field.

Signal modulation in integrated photonic devices requires optical phase control that can be exercised by manipulating the effective refractive index of the waveguide. Different strategies have been considered for the design of SiN-based optical modulators. In Ref. [49], it is proposed the fabrication of a ring microresonator consisting of a MoS layer structure on a SiN substrate coated by the IL $[DEME][NTf_2]$ to control the charge doping processes. Direct and inverse bias voltages change the effective index of the waveguide, producing a change in the transmission spectra due to a redshift or a blueshift of the resonance wavelength.

The refractive index is a property sensitive to enviromental factors such as humidity, which induces water absorption in some ILs. Therefore, variations in the refractive index can be used to estimate the amount of water absorbed by an IL. In Ref. [51], a neural network-based model was developed to estimate the purity of an IL from the molecular mass, the nominal refractive index and the measured refractive index. It was applied to the ILs $[C_4C_1im][BF_4]$ and $[C_4C_1im][C_1SO_4]$. Measurable differences in refractive index were obtained when the water content was greater than 1% by weight.

On the other hand, Kaneko et al. [52] studied with a simpler model the effects of the presence of a known amount of water on the refractive index. An indirect application of their study is the determination of the water mole fraction from the values of the dry IL and the IL-water mixture. It is worth to note that most standardized refractive index measurement systems do not usually have sufficient sensitivity to detect the presence of impurities or very small amounts of water, being necessary to resort to more sensitive techniques such as surface plasmon resonance sensors that work well detecting refractive index variations that can be of the order of 10^{-5} or 10^{-6} RIU.

5. Conclusions

The initial measurements of optical properties in ILs aimed to provide a comprehensive physicochemical characterization of these emerging materials. As the number of experimental measurements increased, namely those of the refractive index at the sodium D line, the possibility of modifying their optical response through structural changes became apparent. This goal has been the focus of several recent experimental and computational studies. From an experimental perspective, refractive index measurements have been expanded beyond single-wavelength to include wider spectral regions, allowing for the study of its wavelength dependence in the visible, ultraviolet, and infrared ranges. In consequence, these studies have investigated the impact of different ion combinations on refractive index, not only at the sodium D line, but also across the entire refractive index curve. From a computational perspective, many publications have focused on predicting the refractive index of specific ion

combinations, which lays the groundwork for future experimental work. The computational efforts were based on two different approaches. The first one exploits the additivity of electronic polarizability in terms of atoms or molecular units to build the overall electronic polarizability of new ILs and their refractive index via the Lorentz-Lorenz equation. The other approach involves applying artificial intelligence algorithms to large amounts of experimental data to create models with the ability to predict the refractive index of new ILs. These experimental and computational efforts to unravel the relationships between molecular structure and refractive index in ILs, has led to an increase in the number of works investigating their potential optical applications. As a result of it, ILs are being studied as optical materials in photonic fields such as optical communications and sensing, in addition to early-proposed applications such as high refractive index immersion fluids or variable focal length liquid lenses.

Abbreviations

Cation	
$[C_kC_1im]^+$	1-alkyl-3-methylimidazolium
$[BzC_1im]^+$	1-benzyl-3-methylimidazolium
$[AllC_1im]^+$	1-allyl-3-methylimidazolium
$[AllC_1C_1im]^+$	1-allyl-2,3-dimethylimidazolium
$[C_4C_1imI_2]^+$	4,5-diiodo-1-butyl-3-methylimidazolium
$[C_2CNC_4im]^+$	3-(3-butyl-1H-imidazol-3-ium-1-yl)propanenitrile
$[C_2CNAim]^+$	3-(3-allyl-1H-imidazol-3-ium-1-yl)propanenitrile
$[C_2CNBzim]^+$	3-(3-benzyl-1H-imidazol-3-ium-1-yl) propanenitrile
$[C_2CNHeim]^+$	3-[3-(2-hydroxyethyl)-1H-imidazol-3-ium-1-yl]propanenitrile
$[C_2OC_2C_1im]^+$	1-ethoxyethyl-3-methylimidazolium
$[C_4(C_1im)_2]^{2+}$	1,1-bis(3-methylimidazolium-1-yl) butylene
$[N_{kk}]^+$	di(alkyl)ammonium
$[N_{4444}]^+$	tetra(butyl)ammonium
$[DEME]^+$	diethylmethyl(2-methoxyethyl)ammonium
$[P_{444k}]^+$	tri(butyl)-alkyl-phosphonium
$[P_{kkkk}]^+$	tetra(alkyl)phosphonium
$[P_{666,14}]^+$	tri(hexyl)tetradecylphosphonium
$[P_{ppp6}]^+$	hexyltryphenyl-phosphonium
$[P_{i(444)1}]^+$	tri(isobutyl) methylphosphonium
$[C_1py]^+$	1-methylpyridinium
$[piC_5py]^{2+}$	1-(1-methypiperidinium-1-yl) pentane-(1-pyridinium)
$[Ch]^+$	cholinium
$[C_1C_kMor]^+$	N-alkyl-N-methylmorpholinium
Anion	
$[I_5]^-$	pentaiodide
$[PF_6]^-$	hexafluorophosphate
$[BrI_2]^-$	bromodiiodide
$[HSO_4]^-$	hydrogensulfate
$[C_1SO_3]^-$	methanesulfonate
$[C_1SO_4]^-$	methylsulfate
$[Bz\text{-}I\text{-}SO_3]^-$	2-iodobenzenesulfonate
$[OTf]^-$	trifluoromethanesulfonate

$[NTf_2]^-$	bis(trifluoromethylsulfonyl)imide
$[SCN]^-$	thiocyanate
$[MOPSO]^-$	2-hydroxy-3-morpholinopropanesulfonate
$[BES]^-$	2-(bis(2-hydroxyethyl)amino)ethanesulfonate
$[TAPSO]^-$	N-[tris(hydroxymethyl)methyl]-3-amino-2-hydroxypropane-sulfonate
$[CAPSO]^-$	3-(cyclohexylamino)-2-hydroxypropanesulfonate
$[\rho\text{-TSA}]^-$	paratoluene sulfonate
$[(R\text{-}O)_2PO_2]^-$	di(alkyl)phosphate
$[C_1C_1OPO_2]^-$	methyl-methylphosphonate
$[C_1OHPO_2]^-$	methylphosphonate
$[Ac]^-$	acetate
$[Ala]^-$	N-acetyl-L-alaninate
$[Val]^-$	N-acetyl-L-valinate
$[Leu]^-$	N-acetyl-L-leucinate
$[Ile]^-$	N-acetyl-L-isoleucinate
$[C_kCO_2]^-$	alkanoate
$[CF_3COO]^-$	trifluoroacetic acid
$[Tos]^-$	tosylate
$[Sac]^-$	saccharinate
$[N(CN)_2]^-$	dicyanamide

Author details

Yago Arosa[1], Carlos Damián Rodríguez-Fernández[2], Elena López Lago[1] and Raúl De la Fuente[1*]

1 Departamento de Física Aplicada e Instituto de Materiais (iMATUS), Universidade de Santiago de Compostela, Spain

2 Departamento de Física e Ciencias da Terra, Universidade da Coruña, Spain

*Address all correspondence to: raul.delafuente@usc.es

References

[1] Bonhôte P, Dias A-P, Papageorgiou N, Kalyanasundaram K, Grätzel M. Hydrophobic, highly conductive ambient-temperature molten salts. Inorganic Chemistry. 1996;**35**(5): 1168-1178

[2] Huddleston JG, Visser AE, Reichert WM, Willauer HD, Broker GA, Rogers RD. Characterization and comparison of hydrophilic and hydrophobic room temperature ionic liquids incorporating the imidazolium cation. Green Chemistry. 2001;**3**(4): 156-164

[3] De Los Ríos AP, Fernández FJH. Ionic Liquids in Separation Technology. Amsterdam, Netherlands: Elsevier; 2014

[4] Kayama Y, Ichikawa T, Ohno H. Transparent and colourless room temperature ionic liquids having high refractive index over 1.60. Chemical Communications. 2014;**50**(94): 14790-14792

[5] Gonfa G, Bustam MA, Muhammad N, Khan AS. Evaluation of thermophysical properties of functionalized imidazolium thiocyanate based ionic liquids. Industrial and Engineering Chemistry Research. 2015;**54**(49):12428-12437

[6] Ullah S, Al-Sehemi AG, Assiri MA, Mukhtar A, Ayoub M, Bustamb MA, et al. Experimental investigation and modeling of the density, refractive index, and dynamic viscosity of 1-propyronitrile-3-butylimidazolium dicyanamide. Journal of Molecular Liquids. 2020;**302**:112470

[7] Bhattacharjee A, Lopes-da-Silva JA, Freire MG, Coutinho JAP, Carvalho PJ. Thermophysical properties of phosphonium-based ionic liquids. Fluid Phase Equilibria. 2015;**400**:103-113

[8] Rodil E, Arce A, Arce A, Soto A. Measurements of the density, refractive index, electrical conductivity, thermal conductivity and dynamic viscosity for tributylmethylphosphonium and methylsulfate based ionic liquids. Thermochimica Acta. 2018;**664**:81-90

[9] Othman Zailani NHZ, Yunus NM, Ab Rahim AH, Bustam MA. Thermophysical properties of newly synthesized ammonium-based protic ionic liquids: Effect of temperature, anion and alkyl chain length. Processes. 2020;**8**(6):742

[10] Lee SY, Vicente FA, Coutinho JAP, Khoiroh I, Show PL, Ventura SPM. Densities, viscosities, and refractive indexes of good's buffer ionic liquids. Journal of Chemical & Engineering Data. 2016;**61**(7):2260-2268

[11] Marcinkowski Ł, Szepiński E, Milewska MJ, Kloskowski A. Density, sound velocity, viscosity, and refractive index of new morpholinium ionic liquids with amino acid-based anions: Effect of temperature, alkyl chain length, and anion. Journal of Molecular Liquids. 2019;**284**:557-568

[12] Khan AS, Man Z, Arvina A, Bustama MA, Nasrullah A, Ullah Z, et al. Dicationic imidazolium based ionic liquids: Synthesis and properties. Journal of Molecular Liquids. 2017;**227**:98-105

[13] Branco ASH, Calado MS, Fareleira JMNA, Visak ZP, Canongia Lopes JN. Refraction index and molar refraction in ionic liquid/PEG200 solutions. Journal of Solution Chemistry. 2015;**44**:431-439

[14] Wang J, Song H, Yang X, Zou W, Chen Y, Duan S, et al. Density, viscosity, refraction index and excess properties of

binary mixtures of 1-(1-methypiperidinium-1-yl) pentane-(1-pyridinium) bis(trifluoromethane) sulfonamide with acetonitrile at T= (293.15 to 323.15) K. Korean Journal of Chemical Engineering. 2016;**33**(8): 2460-2468

[15] Calixto S, Rosete-Aguilar M, Sanchez-Marin FJ, Torres-Rocha OL, Prado EMM, Calixto-Solano M. Optofluidic compound lenses made with ionic liquids. In: Applications of Ionic Liquids in Science and Technology. London, UK: InTech; 2011

[16] Nóvoa-López JA, López Lago E, Domínguez-Pérez M, Troncoso J, Varela LM, de la Fuente R, et al. Thermal refraction in ionic liquids induced by a train of femtosecond laser pulses. Optics and Laser Technology. 2014;**61**:1-7

[17] Chiappe C, Margari P, Mezzetta A, Pomelli CS, Koutsoumpos S, Papamichael M, et al. Temperature effects on the viscosity and the wavelength-dependent refractive index of imidazolium-based ionic liquids with a phosphorus-containing anion. Physical Chemistry Chemical Physics. 2017; **19**(12):8201-8209

[18] Mero A, Guglielmero L, D'Andrea F, Pomelli CS, Guazzelli L, Koutsoumpos S, et al. Influence of the cation partner on levulinate ionic liquids properties. Journal of Molecular Liquids. 2022;**354**: 118850

[19] Wu X, Muntzeck M, de los Arcos T, Grundmeier G, Wilhelm R, Wagner T. Determination of the refractive indices of ionic liquids by ellipsometry, and their application as immersion liquids. Applied Optics. 2018;**57**(31):9215

[20] Rola K, Zajac A, Czajkowski M, Fiedot-Tobola M, Szpecht A, Cybinska J, et al. Electron beam patterning of polymerizable ionic liquid films for application in photonics. Langmuir. 2019;**35**(37):11968-11978

[21] Elmahdy MM, Fahmy T, Aldhafeeri KA, Ibnouf EO, Riadi Y. Optical and antibacterial properties of 1-butyl-3-methylimidazolium ionic liquids with trifluoromethanesulfonate or tetrafluoroborate anion. Materials Chemistry and Physics. 2021;**264**:124369

[22] Arosa Y, Rodríguez-Fernández CD, López Lago E, Amigo A, Varela LM, Cabeza O, et al. Refractive index measurement of imidazolium based ionic liquids in the Vis-NIR. Optical Materials. 2017;**73**:647-657

[23] Arosa Y, Algnamat BS, Rodríguez CD, López Lago E, Varela LM, de la Fuente R. Modeling the temperature-dependent material dispersion of imidazolium-based ionic liquids in the VIS-NIR. Journal of Physical Chemistry C. 2018;**122**(51):29470-29478

[24] Algnamat BS, Arosa Y, López Lago E, de la Fuente R. An inspection of the dispersive properties of imidazolium-based ionic liquids in the Vis-NIR. Optical Materials. 2020;**102**: 109764

[25] Rodríguez Fernández CD, Arosa Y, Algnamat B, López Lago E, de la Fuente R. An experimental and computational study on the material dispersion of 1-alkyl-3-methylimidazolium tetrafluoroborate ionic liquids. Physical Chemistry Chemical Physics. 2020;**22**(25): 14061-14076

[26] Gardas RL, Coutinho JAP. Group contribution methods for the prediction of thermophysical and transport properties of ionic liquids. AICHE Journal. 2009;**55**(5):1274-1290

[27] Sattari M, Kamari A, Mohammadi AH, Ramjugernath D. A group contribution method for estimating the refractive indices of ionic liquids. Journal of Molecular Liquids. 2014;**200**:410-415

[28] Izgorodina EI, Forsyth M, MacFarlane DR. On the components of the dielectric constants of ionic liquids: Ionic polarization? Physical Chemistry Chemical Physics. 2009;**11**(14):2452

[29] Bica K, Deetlefs M, Schröder C, Seddon KR. Polarisabilities of alkylimidazolium ionic liquids. Physical Chemistry Chemical Physics. 2013;**15**(8): 2703

[30] Bernardes CES, Shimizu K, Canongia Lopes JN, Marquetand P, Heid E, Steinhauser O, et al. Additive polarizabilities in ionic liquids. Physical Chemistry Chemical Physics. 2016;**18**(3): 1665-1670

[31] Heid E, Heindl M, Dienstl P, Schröder C. Additive polarizabilities of halides in ionic liquids and organic solvents. The Journal of Chemical Physics. 2018;**149**(4):044302

[32] Rodríguez-Fernández CD, López Lago E, Schröder C, Varela LM. Non-additive electronic polarizabilities of ionic liquids: Charge delocalization effects. Journal of Molecular Liquids. 2022;**346**:117099

[33] Koutsoumpos S, Chronaki M, Tsonos C, Karakasidis T, Guazzelli L, Mezzetta A, et al. On the application of the Wildman-Crippen model to ionic liquids. Results in Materials. 2022;**16**: 100350

[34] Wildman SA, Crippen GM. Prediction of physicochemical parameters by atomic contributions. Journal of Chemical Information and Computer Sciences. 1999;**39**(5):868-873

[35] Venkatraman V, Raj JJ, Evjen S, Lethesh KC, Fiksdahl A. In silico prediction and experimental verification of ionic liquid refractive indices. Journal of Molecular Liquids. 2018;**264**: 563-570

[36] Esmaeili A, Hekmatmehr H, Atashrouz S, Madani SA, Pourmahdi M, Nedeljkovic D, et al. Insights into modeling refractive index of ionic liquids using chemical structure-based machine learning methods. Scientific Reports. 2023;**13**(1):1966

[37] Baskin I, Epshtein A, Ein-Eli Y. Benchmarking machine learning methods for modeling physical properties of ionic liquids. Journal of Molecular Liquids. 2022;**351**:118616

[38] Zhang S, Zhang Q, Zhang Y, Chen Z, Watanabe M, Deng Y. Beyond solvents and electrolytes: Ionic liquids-based advanced functional materials. Progress in Materials Science. 2016;**77**(6):80-124

[39] Borra EF, Seddiki O, Angel R, Eisenstein D, Hickson P, Seddon KR, et al. Deposition of metal films on an ionic liquid as a basis for a lunar telescope. Nature. 2007;**447**(7147): 979-981

[40] Rogers RD, Seddon KR. Ionic Liquids IIIB Fundamentals, Progress, Challenges and Opportunities. Transformations and process, ACS Sympos. Oxford, United Kingdom: Oxford University Press; 2005

[41] Deetlefs M, Shara M, Seddon KR. Refractive indices of ionic liquids. ACS Symposium Series. 2005;**901**:219-233

[42] Guo J, Zhou M, Liu YG, Di K, Li R, Cui W, et al. An all-optical controlled

attenuation effect in an all-fiber system based on ionic liquid-filled photonic bandgap fiber. Physica Scripta. 2019; **94**(11):115508

[43] Abood I, Elshahat S, Ouyang Z. High figure of merit optical buffering in coupled-slot slab photonic crystal waveguide with ionic liquid. Nanomaterials. 2020;**10**(9):1742

[44] Liu Q, Liu Z, Li C, Xie K, Zhu P, Shao B, et al. Highly transparent and flexible iontronic pressure sensors based on an opaque to transparent transition. Advancement of Science. 2020;**7**(10): 2000348

[45] Ohkura M, Takana H, Ohuchi FS, Furukawa R. Fabrication of liquid-core fiber-optic structure for large-area CO_2 sensing using ionic liquids. Journal of Fluid Science and Technology. 2021; **16**(1):JFST0004

[46] Calixto S, Sánchez-Morales ME, Sánchez-Marin FJ, Rosete-Aguilar M, Richa AM, Barrera-Rivera KA. Optofluidic variable focus lenses. Applied Optics. 2009;**48**(12):2308

[47] Hu X, Zhang S, Qu C, Zhang Q, Lu L, Ma X, et al. Ionic liquid based variable focus lenses. Soft Matter. 2011; **7**(13):5941

[48] Hu X, Zhang S, Liu Y, Qu C, Lu L, Ma X, et al. Electrowetting based infrared lens using ionic liquids. Applied Physics Letters. 2011;**99**(21):213505

[49] Chen H, Zhao Z, Zhang Z, Wang G, Li J, Shang Z, et al. Heterogeneous integrated phase modulator based on two-dimensional layered materials. Photonics Research. 2022;**10**(6):1401

[50] Wang Y, Swain GM, Blanchard GJ. Charge-induced birefringence in a room-temperature ionic liquid. The Journal of Physical Chemistry. B. 2021;**125**(3): 950-955

[51] Díaz-Rodríguez P, Cancilla JC, Matute G, Chicharro D, Torrecilla JS. Inputting molecular weights into a multilayer perceptron to estimate refractive indices of dialkylimidazolium-based ionic liquids—A purity evaluation. Applied Soft Computing. 2015;**28**: 394-399

[52] Kaneko K, Yoshimura Y, Shimizu A. Water concentration dependence of the refractive index of various ionic liquid-water mixtures. Journal of Molecular Liquids. 2018;**250**:283-286